

Complex Optical–X-ray Correlations in the Narrow-Line Seyfert 1 Galaxy NGC 4051

O. Shemmer,^{1*} P. Uttley,^{2,3} H. Netzer¹ and I. M. McHardy²

¹*School of Physics and Astronomy and the Wise Observatory, The Raymond and Beverly Sackler Faculty of Exact Sciences, Tel-Aviv University, Tel-Aviv 69978, Israel*

²*Department of Physics and Astronomy, University of Southampton, Southampton SO17 1BJ, United Kingdom*

³*Visiting astronomer, Tel-Aviv University, Wise Observatory*

Accepted 2003 May 7. Received 2002 December 13; in original form 2002 December 13

ABSTRACT

This paper presents the results of a dense and intensive X-ray and optical monitoring of the narrow-line Seyfert 1 galaxy NGC 4051 carried out in 2000. Results of the optical analysis are consistent with previous measurements. The amplitude of optical emission line variability is a factor of two larger than that of the underlying optical continuum, but part or all of the difference can be due to host-galaxy starlight contamination or due to the lines being driven by the unseen UV continuum, which is more variable than the optical continuum. We measured the lag between optical lines and continuum and found a lower, more accurate broad line region size of 3.0 ± 1.5 light days in this object. The implied black hole mass is $M_{BH} = 5_{-3}^{+6} \times 10^5 M_{\odot}$; this is the lowest mass found, so far, for an active nucleus. We find significant evidence for an X-ray–optical (XO) correlation with a peak lag $\lesssim 1$ day, although the centroid of the asymmetric correlation function reveals that part of the optical flux varies in advance of the X-ray flux by 2.4 ± 1.0 days. This complex XO correlation is explained as a possible combination of X-ray reprocessing and perturbations propagating from the outer (optically emitting) parts of the accretion disc into its inner (X-ray emitting) region.

Key words:

galaxies: active – galaxies: individual: NGC 4051 – X-rays: galaxies

1 INTRODUCTION

Correlations between different parts of the spectral energy distribution in active galactic nuclei (AGN), have been utilized in the past decade as an important tool to probe and map the deepest components of the central engine’s energy source. Several attempts have aimed at finding a connection between X-ray and optical light curves, in order to follow the source and location of the X-ray emission. Such attempts have been carried out in the past decade as part of AGN multiwavelength monitoring campaigns (e.g. Done et al. 1990, Nandra et al. 1998, 2000, Edelson et al. 2000, Maoz, Edelson & Nandra 2000, Peterson et al. 2000; P00, Shemmer et al. 2001; see also Maoz et al. 2002 for a brief summary of previous campaigns). So far, reliable determinations of X-ray–optical (XO) correlations are few and far between. In most cases where a strong correlation was found, the X-ray

and optical light curves appeared to vary simultaneously, i.e. practically with zero lag. For example, on long timescales (days–months) all attempts to find XO lags have failed (e.g. Clavel et al. 1992 in NGC 5548, Done et al. 1990 and P00 in NGC 4051, Shemmer et al. 2001 in Ark 564, and Maoz et al. 2002 in NGC 3516). Even on shorter timescales (hours) XO correlations and lags are rare (e.g. Edelson et al. 1996 in NGC 4151, but see also Edelson et al. 2000 for no XO correlation in NGC 3516).

One exception is NGC 7469 (Nandra et al. 1998, 2000), in which a significant correlation was found between the optical/UV continuum and the X-ray flux that followed it with a ~ 4 days lag, including periods when increasing X-ray flux led decreasing UV flux by a similar lag. This complex behaviour ruled out two possible scenarios: UV seed photons that are Compton up-scattered to produce X-rays in a putative corona (UV leading X-ray; e.g. Haardt & Maraschi 1991, 1993) or UV radiation that is produced by reprocessed X-ray photons (X-ray leading UV; e.g. Stern et al. 1995). Uttley et

* ohad@wise.tau.ac.il

al. (2003) find a very strong correlation between long time-scale (months) X-ray and optical variations in NGC 5548, but constrain any lag to be less than 15 days. Another success in finding an XO correlation was during the Ark 564 campaign, when an X-ray flare was followed ~ 2 days later by an optical flare (Shemmer et al. 2001) and was interpreted in terms of reprocessing models.

The successful detection of an optical response to an X-ray flare in Ark 564, a narrow-line Seyfert 1 (NLS1) galaxy, has motivated us to search for similar behaviour in other NLS1s that we have been monitoring as part of a larger project. Since one of the more pronounced characteristics of NLS1s is the intense X-ray variation (e.g. Boller, Brandt, & Fink 1996; Leighly 1999a, 1999b), which is at least one order of magnitude larger in amplitude than in ‘normal’ Seyfert 1 galaxies, we assumed that detection of XO connections will be more frequent and more pronounced in this sub-class of AGN. One difficulty though, appears to be the fact that the persistent large and rapid X-ray variability in NLS1s (flux variations of a factor of two or more on timescales of minutes/hours) is contrasted by the very low variability exhibited by the optical band. NLS1s differ markedly from ‘normal’ broad-line Seyfert 1 galaxies (e.g. NGC 7469; Nandra et al. 1998, 2000) in this respect by varying strongly in the X-ray while showing little or no variability in the optical/UV band (e.g. Ark 564; Shemmer et al. 2001).

NGC 4051 is a nearby ($z = 0.0023$), low luminosity ($\sim 10^{42}$ erg s $^{-1}$), NLS1 (FWHM(H β)=1110 km s $^{-1}$) that had been studied extensively across the spectrum (e.g. Uttley et al. 1999, Lamer et al. 2002, Collinge et al. 2001 and references therein) and has shown optical variability amplitudes of up to $\sim 10\%$ in flux (Done et al. 1990, P00). In 2000 we carried out a dense and continuous X-ray and optical monitoring campaign on NGC 4051. Our major goal aimed at finding a temporal relationship between the variations observed in the two bands. In this paper we present the results of this campaign. Section 2 presents the observational data and their reduction. In § 3 we present the results of the time series analysis and in § 4 discuss its implications. Section 5 summarizes our main conclusions.

2 OBSERVATIONS AND DATA REDUCTION

2.1 The Optical Band

NGC 4051 was monitored spectrophotometrically during May–July 2000 at the Tel-Aviv University Wise Observatory (WO). The observations were carried out with the Faint Object Spectrograph & Camera on top of the WO 1m telescope. We used a 10”-wide long-slit and a 600 lines mm $^{-1}$ grism. A Tektronix 1024 \times 1024 pixel back-illuminated CCD was used as the detector. Reduction of the data was carried out in the usual manner using IRAF † with its SPECRED, ONEDSPEC and TWODSPEC packages. In order to reduce light contamination from the host galaxy while not lowering the

† IRAF (Image Reduction and Analysis Facility) is distributed by the National Optical Astronomy Observatories, which are operated by AURA, Inc., under cooperative agreement with the National Science Foundation.

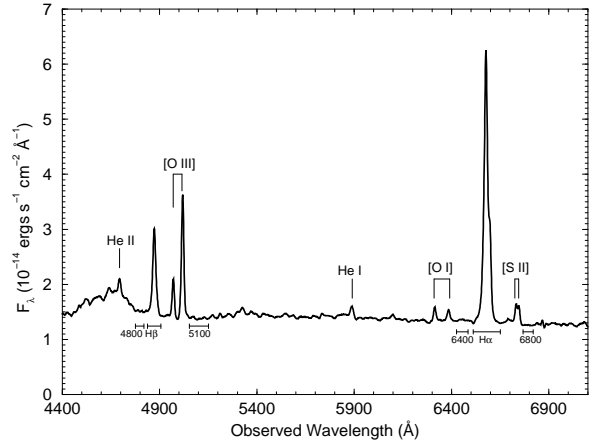


Figure 1. Mean spectrum of NGC 4051 observed at WO. The continuum and line measurement bins are marked.

S/N ratio, we extracted the spectrum using an 8” extraction window. Spectrophotometric calibration of the nucleus of NGC 4051 was carried out using the technique in which a nearby comparison star is observed simultaneously with the object of interest inside a wide slit. This technique of using a local comparison star is described in detail by Maoz et al. (1990, 1994) and produces high relative spectrophotometric accuracy. Each spectroscopic observation consisted of two 15 minute exposures of NGC 4051 and its comparison star. The consecutive galaxy/star flux ratios were compared to test for systematic errors in the observations and to clean cosmic rays. We discarded pairs of data points with ratios larger than $\sim 5\%$ and verified that the comparison star is non-variable to within $\sim 2\%$ by means of differential photometry of other stars in the field, carried out before this campaign began. As a result, 31 good-quality spectra remained. The spectra were calibrated to an absolute flux scale by multiplying each galaxy/star ratio by a spectrum of the comparison star that was flux calibrated by applying a characteristic WO extinction curve and CCD sensitivity function, that do not change considerably from night to night. The absolute flux calibration has an uncertainty of $\sim 10\%$, which is not shown in the error bars of our light curves. The error bars reflect only the differential uncertainties, which are of order 2%-3%. By measuring the [O III] λ 5007 fluxes in our spectra, we verified that the differential uncertainty level is consistent with the night-to-night scatter in this narrow emission line light curve (which is expected to maintain a constant flux level). We measured the mean flux in narrow line-free continuum bands close to H α and H β (see Figure 1) and the integrated flux of both emission lines in each spectrum. Two of the resulting light curves (together with the X-ray light curve, see §§ 2.2) are plotted in Figure 2.

2.2 X-ray Observations

NGC 4051 was intensively monitored by the *Rossi X-ray Timing Explorer (RXTE)* in May–July 2000, as part of an ongoing campaign to measure its broad band X-ray variability power spectrum (M c Hardy et al., in preparation). The intensive monitoring program consisted of 251 observations, each of exposure ~ 1 ks, obtained at roughly 6-hourly in-

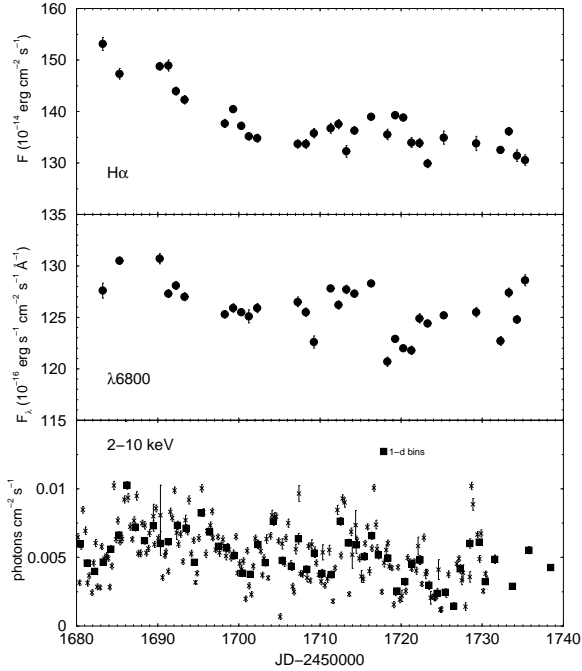


Figure 2. NGC 4051 light curves. From top to bottom: H α flux, continuum flux density at the narrow 6800Å band, and *RXTE* 2–10 keV flux (small 'x's with error bars). The X-ray data were also binned in one-day intervals (filled squares).

intervals from 2000 May 1 to July 5. We used data from the *RXTE* Proportional Counter Array, applying standard good time interval selection criteria and using all available Proportional Counter Units (PCUs; top layer only) to extract a spectrum for each observation. Using *XSPEC*, we fitted each spectrum with a simple power law plus Galactic absorption model, in order to obtain an estimate of the 2–10 keV photon flux which is robust to changes in instrument gain and number of PCUs used (see Lamer et al. 2002 for further details of data reduction and spectral fitting).

3 TIME SERIES ANALYSIS

3.1 Variability

The fractional variability, F_{var} , (Rodríguez-Pascual et al. 1997) of a light curve is defined as

$$F_{var} = \sqrt{\frac{S^2 - \langle \sigma_{err}^2 \rangle}{\langle X \rangle^2}}, \quad (1)$$

where S^2 is the total variance of the light curve, σ_{err}^2 is the mean error squared, and $\langle X \rangle^2$ is the mean flux squared. The uncertainty on F_{var} is (Edelson et al. 2002):

$$\sigma_{F_{var}} = \frac{S^2}{\sqrt{2N} F_{var} \langle X \rangle^2}. \quad (2)$$

A list of F_{var} values calculated for the optical and X-ray light curves appears in Table 1, where it is apparent that the X-ray variability is an order of magnitude larger than

Table 1. Fractional Variability

Band	$F_{var}[\%]$
2–10 keV	44.9 ± 2.0
$\lambda 4800$	3.4 ± 0.5
H β	7.8 ± 1.2
$\lambda 5100$	3.4 ± 0.5
$\lambda 6400$	1.8 ± 0.3
H α	4.0 ± 0.5
$\lambda 6800$	1.9 ± 0.3

the optical variability over the same time interval[‡]. It is also apparent that within the optical band itself, the emission line variations are about twice as large as the underlying optical continuum. This discrepancy may be attributable to contamination of the spectrum by host-galaxy starlight, that tends to reduce the apparent optical continuum fluctuations. For example, Done et al. (1990) estimated respective *B* and *I* band contributions due to NGC 4051 host-galaxy starlight of 33% and 37% of the observed continuum, for a 6'' aperture. Since we use a larger aperture (10'' slit width and 8'' extraction region perpendicular to that), the contribution due to host galaxy starlight may approach the 50% level required to explain the factor of ~ 2 difference in line and continuum variability amplitudes. We tested this by analyzing images of the galaxy taken in the *B* band at WO. By scaling a PSF of other stars in the galaxy's field to the galaxy's nucleus, and then subtracting it from the nucleus, we found that the difference in flux is 15% in a 10'' by 8'' aperture. In other words, the starlight flux contribution to our spectroscopic aperture is at least 15%, which is not a meaningful lower limit due to the limited seeing conditions. To ultimately test the 'host-galaxy starlight contamination' scenario it is better to examine UV continuum variations, since those are free from such contamination. Examination of archival *IUE* spectra taken between 1978 and 1994 shows periods of large and long-term (years) UV variability, with amplitudes that are much larger than those of the optical emission lines. However, the very large errors in the data prevent us from obtaining F_{var} for the UV continuum. We conclude that in spite of our inability to quantitatively point at the source for the larger optical emission line variability, fluctuations in the UV continuum, which are the most likely drivers of those variations, remain a probable explanation that should be further checked with better data than we currently have.

3.2 Cross-Correlations

The X-ray light curve shows strong short time-scale variations which are not reflected in the optical light curves (as previously noted by Done et al. 1990 and P00), so to obtain a

[‡] Even though the sampling patterns of both X-ray and optical light curves are different, both have a similar length and a similar exposure time (~ 10 min.) for each data point. This allows us to directly compare the F_{var} values of the unbinned X-ray light curve to that of the optical. The F_{var} of the 1-d bin X-ray light curve is $35.3 \pm 3.1\%$ and even though it might seem more intuitive to compare this to the optical value, it is technically incorrect since binning the X-rays smooths out the $\lesssim 1$ d variations that contribute to the optical light curve.

better comparison with the optical variations we smoothed out the rapid X-ray variability by binning the X-ray light curve into 1 day bins (see Figure 2) before cross-correlating with the unbinned optical data (which is sampled at \sim daily intervals). To derive the cross-correlation function (CCF) between two light curves (the first assumed to be the driving light curve and the second assumed to be the responding light curve) we utilized the Discrete Correlation Function (DCF) method (Edelson & Krolik 1988). For each pair of light curves, we measured the DCF in the lag range 0 ± 10 d, binning in 1 day lag bins (at larger lags there are fewer pairs of light curve points per lag bin so that spurious peaks in the CCF are much more common). Peak values (r_{\max}) and corresponding peak lags (τ_{peak}) were determined, together with the lag centroid (τ_{cent}), which is a measure of the ‘centre of mass’ of the lag peak, and thus takes account of asymmetries in the correlation. The centroid is determined by summing the CCF values in the range either side of τ_{peak} where the CCF value $r > 0.8r_{\max}$. The uncertainties on the lags (peak and centroid) were estimated using the Flux Randomization/Random Subset Selection (FR/RSS) method (Peterson et al. 1998). The CCFs for the most important correlations are plotted in Fig. 3 and parameters of each correlation are shown in Table 2.

At face-value, the correlations shown in Table 2 appear to be significant, with correlation coefficients larger than one would expect if the data were randomly distributed and uncorrelated. However, the light curves presented here are not random (white-noise) data sets: adjacent data points are correlated with one another to produce variations on a range of time-scales and are consistent with red-noise processes. As such, the correlations between two light curves are driven by only a few events (flares or dips) in each light curve, and it is possible that apparent correlations could be seen even where none exist, simply because the events in two uncorrelated light curves happen to match up by chance. To assign a reliable significance to the correlations, we must simulate uncorrelated red-noise light curves with similar variability properties to the observed light curves, and determine the frequency of spurious correlations. A similar Monte Carlo method to assess the significance of the XO correlation in NGC 5548 has been applied by Uttley et al. (2003). We outline the method here:

1. Simulate two continuous red-noise light curves, of time resolution 0.01 days and length 16384 bins (i.e. 163 d, much larger than the 60 d observed duration) using the method of Timmer & Koenig (1995), with different random number sequences to generate each light curve so they are uncorrelated. We assume broken power-law shapes for both optical and X-ray power spectra, with break frequencies at 1 d^{-1} and power-law slopes above the break of -1.5 and -2 for X-ray and optical power spectra respectively and identical slopes of -1 below the break. The X-ray power-spectral shape is chosen to approximate that measured by much more extensive *RXTE* and *XMM* data sets (M^cHardy et al., in preparation), while the optical power-spectral shape (which is assumed to be the same for continuum and lines) is chosen to reproduce the relatively low variability on short time-scales and mimic the finding in NGC 5548 that the optical and X-ray power spectral shapes differ only at high frequencies (Utt-

ley et al. 2003)[§]. Power-spectral amplitudes are chosen so that the integrated power of the underlying power spectrum gives the observed light curve variance, after observational noise is subtracted (see Uttley, M^cHardy & Papadakis 2002 for further discussion of light curve simulation, as applied to the measurement of power spectra).

2. Apply observational noise to the simulated light curves, by adding to each simulated data point a random deviate of mean zero and variance equal to the average squared error of the corresponding light curve.

3. Resample the simulated light curves to the observed sampling patterns and rebin the simulated, resampled X-ray light curve to 1 d bins.

4. Measure the DCF of the pair of simulated, uncorrelated light curves, and search for a peak value, r_{\max} , as outlined above for the observed light curves. Search within lags of ± 10 days, allowing adequate overlap between the two light curves.

5. Repeat steps 1-4 1000 times, and count the number of times that the simulated r_{\max} exceeds the observed r_{\max} , to yield the significance of the observed correlation.

For example, for the X-ray- $\lambda 6800$ correlation, we observed a maximum correlation coefficient of $r_{\max} = 0.65$. We counted 40 out of 1000 simulated, uncorrelated light curves with $r_{\max} > 0.65$, implying that the observed correlation is significant at the 96% confidence level (i.e. just over 2σ). The estimated significance of each correlation shown in Table 2, is based on such simulations.

We note that our Monte Carlo approach shows that the actual significance of the correlations is considerably less than would be expected from white-noise data given the same values of r_{\max} . However, all the optical continuum-continuum and line-line correlations are significant at better than 95% confidence, as are the XO correlations. The optical continuum-line correlations are not significant, but this represents a limitation of the existing data set which contains few events in each light curve (and some additional scatter which weakens the correlation). Longer data sets confirm that the optical continuum-line correlation is real (Peterson et al. 2000). We stress however that the questions of the significance of a correlation, and the significance of lags measured between two light curves are not the same. The significance of a correlation can be determined by testing the null-hypothesis that the light curves are uncorrelated. However, in order to determine the significance of any lag, one must assume that the light curves are indeed correlated (as is implicit in the FR/RSS method of lag error estimation); in that case the quality of sampling is important to constrain the lag, rather than the number of ‘events’ in the light curve. Therefore we can still measure lags which are well constrained, even though the correlation itself is not formally significant.

[§] To ensure that our significance estimates are not strongly dependent on optical power-spectral shape, which is ill-defined, we also tested light curves with break frequency as low as 0.01 d^{-1} and slope above the break as steep as -2.5, and find no significant deviation from the estimates we present here.

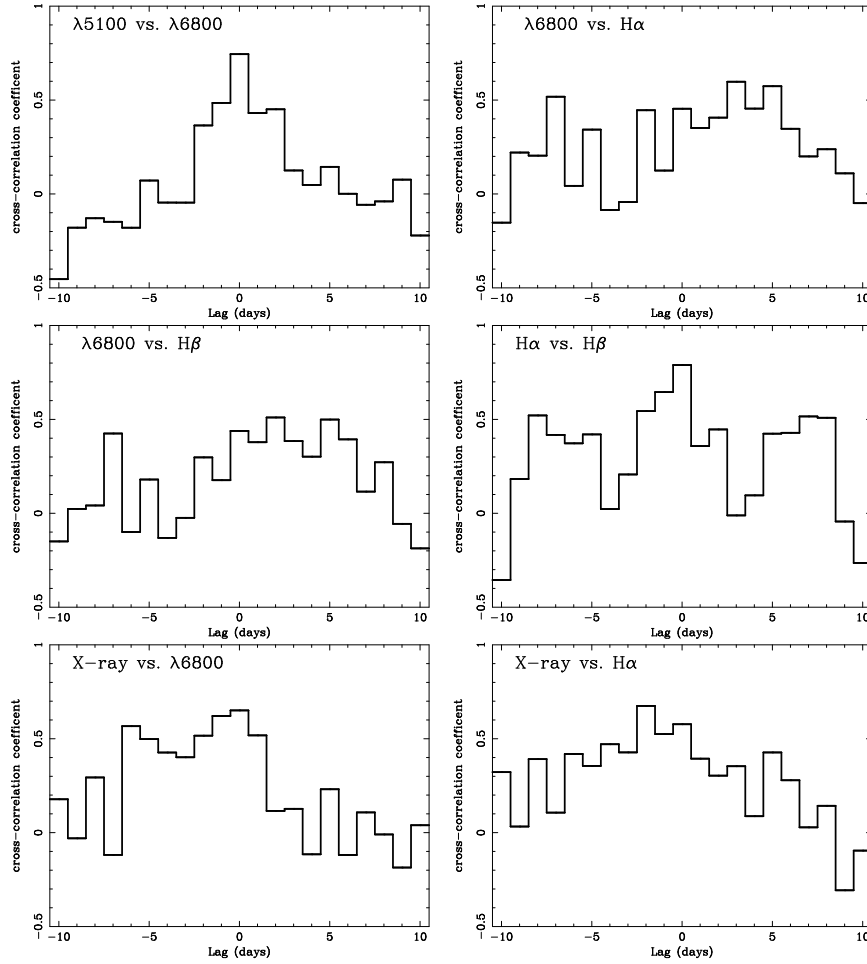


Figure 3. X-ray and optical correlations (see Table 2 for parameters of the correlations). Positive lags imply the second light curve lags the first. Note that although error bars are commonly plotted on DCFs, we do not plot them here as they are meaningless for red-noise data, since errors in the DCF are not independent.

Table 2. NGC 4051 Cross-Correlation Results.

Bands	r_{max}	Significance of r_{max}	τ_{peak} (days)	τ_{cent} (days)
5100Å–6800Å	0.74	0.96	0 ± 1	0.4 ± 0.9
6800Å–H α	0.60	0.85	3.0 ± 1.5	3.1 ± 1.6
X–6800Å	0.65	0.96	0 ± 1	-2.4 ± 1.0
X–H α	0.67	0.97	-2 ± 3	-0.9 ± 1.7
6800Å–H β	0.51	0.69	2.0 ± 2.6	2.0 ± 2.3
H α –H β	0.79	0.98	0 ± 2	-0.9 ± 1.7

4 DISCUSSION

We have monitored NGC 4051 in X-ray and in the optical band on a daily basis for about 60 days in order to find a possible relation between the two bands. Our main observational results are discussed below.

4.1 Optical Line–Continuum Lag

Cross-correlations between the two major Balmer emission-lines and the optical continuum confirm the previously detected lag in this object (P00). We find that H α responds to the continuum variations after 3.0 ± 1.5 days, which is consistent, within the errors, with the $5.92^{+3.13}_{-1.96}$ days reported in P00 for H β . Since we do not detect any lag between H α

and H β , our new line–continuum lag has a lower error, perhaps due to the denser sampling frequency (about once a day) compared with the previous campaign (about once every four days; P00). Moreover, as the observed average flux of NGC 4051 in this study is similar (to within $\sim 10\%$) to that observed during all three phases of the P00 campaign, we suggest that the lower lag we find is not a luminosity effect, but the combined effect of observations and the CCF. By incorporating our lowest error value for the lag (3.0 ± 1.5 days), and $\text{FWHM}(\text{H}\beta) = 1110 \pm 190 \text{ km s}^{-1}$ from P00 into Eq. 5 of Kaspi et al. (2000) for the virial black hole (BH) mass estimate, we obtain $M_{BH} = 5^{+6}_{-3} \times 10^5 M_{\odot}$. Our result is thus consistent, within the errors, with the P00 estimate. The new and lower broad line region (BLR) size we obtained,

$R_{BLR} = 3.0 \pm 1.5$ light days, places NGC 4051 much closer to the best-fit R_{BLR} - L slope produced from reverberation measurements of 34 AGN (see Fig. 6 of Kaspi et al. 2000).

4.2 Optical and X-ray Relation

Inspection of Table 1 shows that the X-ray variability amplitude is about one order of magnitude larger than that of the optical and is ubiquitous in NLS1s (see e.g. Boller et al. 1996, Young et al. 1999). In particular, this result is consistent with the behaviour of NGC 4051 in two previous monitoring campaigns (Done et al. 1990, P00). The striking difference between the variability amplitudes of the X-ray and the optical bands in NLS1s is not yet understood.

Another interesting result is that each optical emission line varies about twice as much as its underlying continuum. This trend was also encountered by Peterson, Crenshaw & Meyers (1985) and by P00. One possible reason for the large F_{var} of the lines might be that the UV and/or the X-ray continua, that are the likely drivers of the line flux, are varying with much larger amplitudes. However, in 1998 the $H\beta$ flux remained unchanged when the X-ray source almost completely turned off and so the highly variable X-ray continuum does not contribute significantly to the Balmer lines production (P00). Large amplitude UV variations do, however, remain a possibility and would be consistent with the very large EUV variations observed by Uttley et al. (2000). The other remaining, and more likely, possibility is that the host-galaxy contribution to the optical continuum is larger than estimated here ($\sim 50\%$; see e.g. the case of NGC 5548, Gilbert & Peterson 2003).

The X-ray and optical light curves are apparently correlated at $> 95\%$ confidence, although the light curves are not simply correlated which would lead to a much clearer peak in the CCF (e.g. see the $\lambda 5100$ - $\lambda 6800$ correlation). The relation between the X-ray and $\lambda 6800$ light curves can be seen by rescaling both light curves (after subtracting their respective means) by their rms variability (i.e. F_{var} multiplied by mean flux), as shown in Figure 4. No lag is introduced into any light curve. The X-ray and optical light curves can be seen to be generally correlated, at least on long time-scales, but there are occasional large discrepancies between the two (which are not attributable to observational noise) which reduce the strength of the observed correlation. The differences between the rescaled light curves in Figure 4 may be attributable to the large amplitude of short-time-scale X-ray variability relative to the amplitude of long-time-scale variations, which implies that the X-ray power spectrum is flatter than the optical power spectrum. Much better signal-to-noise and sampling in both X-ray and optical light curves would be required in order to tell if corresponding short-term variations appear (but at a much weaker level) in the optical light curve.

We find that the peak of the XO cross-correlation is at zero lag but that the centroid of the CCF lies at an optical-to-X-ray lag of 2.4 ± 1.0 days. From simulations we have shown that the probability of exceeding the observed peak cross-correlation coefficient in random data from suitably constructed light curves is 4%.

This result should be compared with two previous attempts to measure XO lags in NGC 4051. The first attempt (Done et al. 1990) found very little variability ($F_{var} < 1\%$)

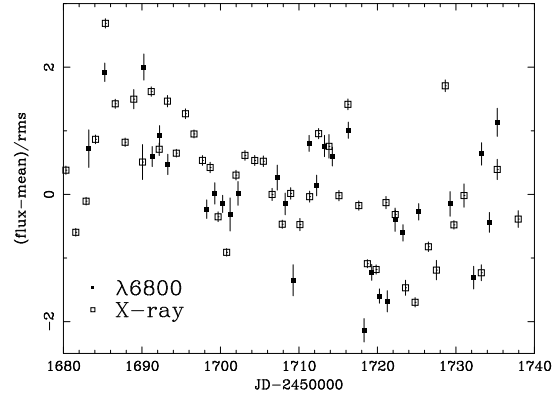


Figure 4. Comparison of X-ray 2–10 keV (open squares) and optical $\lambda 6800$ (filled squares) light curves, renormalised by their respective rms variability (after mean subtraction).

in the optical band in an observational period of a week (and hence no measurable lag) and the second attempt found a good correlation on long time-scales with approximately zero lag (P00). The result of Done et al. (1990) is consistent with our observations as we find that NGC 4051 shows only small-amplitude optical variability on time-scales of a week (see Figure 2). Peterson et al. (2000) were unable to find any XO correlation on short time-scales, probably due to relatively poor X-ray sampling compared to the light curve we present here. On long time-scales, their light curves were smoothed by a 30-day boxcar, thus suppressing any rapid X-ray variations and rendering the detection of a short lag, such as the one we mention here, impossible.

Also of significant interest is the recent result of Mason et al. (2002). In a 130 ks observation of NGC 4051 with XMM-Newton, they found that the 0.1–12 keV X-ray continuum led the $\lambda 2000$ UV continuum, measured with the XMM-Newton optical monitor, by 0.17 days. The significance of that result is similar to that found here. They interpret their observation as optical variability arising from reprocessing of X-ray photons in a region surrounding the central X-ray source.

The fact that the peak of our XO CCF is at zero lag is quite consistent with the result of Mason et al. (2002). Their short observation is not sensitive to the longer timescales which we sample and we are not able to resolve the very short timescales which they sample.

Interestingly, we also find that the XO CCF appears to be asymmetric, in that although it has a zero-lag peak, it has a negative centroid lag, τ_{cent} (i.e. X-rays lag optical). A negative centroid lag and zero peak lag can be reconciled if the variations on timescales longer than a few hours have a different lag, and hence probably a different physical origin, than those on shorter timescales. We can use Monte Carlo simulations to test whether such an observed centroid lag would be expected by chance from perfectly correlated light curves (i.e. light curves with true peak and centroid lag of zero) by counting the number of simulated CCFs with a greater XO lag than observed[¶]. We find that only 2% of

[¶] The light curves are generated as in § 3.2, but using identical random number sequences for light curve generation before resampling and applying Gaussian noise.

simulated pairs of perfectly correlated light curves show centroid lags of greater than 2.4 d, suggesting that the centroid lag and hence observed asymmetry in the CCF is real (as implied by the lag error estimated using the FR/RSS method). However, we caution that the significance of the centroid lag estimated by Monte Carlo simulations is model-dependent: we have only tested the significance of the centroid lag assuming perfectly correlated light curves.

Our putative lag, deduced from the offset position of the centroid of the CCF might, at first thought, be assumed to result from Compton upscattering of UV/optical seed photons to produce X-ray photons (e.g. Haardt & Maraschi 1991, 1993). A similar argument was used by Uttley et al. (2000) for NGC 4051 to explain the very strong correlation between the X-ray and EUV emissions, whose variations are simultaneous to within 1 ks. In that case the size of the X-ray emitting region was calculated to be $\leq 20R_g$. Taking account of the increased spectral difference between the optical and X-ray bands compared to that between the EUV and X-ray bands, and the greater length of the putative lag here, the implied size of the X-ray emitting region would be $\sim 1000R_g$, much larger than deduced previously. It is hard to reconcile such a large size with the rapid X-ray variability. It is also not easy to reconcile an accretion disc of this size (or the hot corona of such a disc) with the observed properties of this source.

An alternative explanation of an X-ray lag is that the optical emitting region is further out in the accretion disk than the X-ray emitting region (which may be a hot corona $< 20R_g$ in size, Uttley et al. 2000). Variations propagating inwards, perhaps at the viscous or diffusion timescale (which in NGC 4051 can be quite short, especially if the disk is thick), would first affect the optical emitting region and, later, the X-ray emitting region. A similar explanation, based on the model for flickering in X-ray binaries suggested by Lyubarskii (1997), is used by Kotov, Churazov and Gilfanov (2001) to explain the energy dependence of the time lags in the X-ray variations in Cyg X-1. Given the many similarities in variability properties of AGN and X-ray binaries (e.g. Uttley et al. 2002, M^cHardy et al., in preparation), such a model might also be applicable to explain the possible X-ray lag in NGC 4051.

5 CONCLUSIONS

Our main conclusions are summarized as follows:

1. Variability amplitudes of our X-ray and optical light curves are consistent with previous observations of NGC 4051. However, despite several good arguments made to explain the observed emission-line variability amplitudes, that are larger by a factor of 2 than the optical continuum variability amplitude, a lack of quantitative evidence remains.

2. Our measured R_{BLR} value is 3.0 ± 1.5 light days, which is about a factor of 2 lower than previous measurements. This implies $M_{BH} = 5_{-3}^{+6} \times 10^5 M_{\odot}$, and places NGC 4051 much closer than before to the best-fit R_{BLR} – L slope of Kaspi et al. (2000). The apparent change in BLR distance is not a luminosity effect, but rather an observational one, since at least the optical flux of the galaxy remained practically constant during all the monitoring campaigns.

3. There is significant evidence for an X-ray/optical correlation close to zero lag (within one day) in NGC 4051. There is also evidence that part of the optical flux varies in advance of the X-ray flux by about 2 days. Although the amplitude of the optical variations is very low, these observations are consistent with X-ray/optical variations seen elsewhere and are probably best explained by a combination of effects including reprocessing of X-ray photons and a physical separation of the main X-ray and optical producing regions. Although Compton up-scattering of optical photons to produce X-ray photons cannot be ruled out, optical photons do not appear to be as important to the seed photon continuum as UV photons.

ACKNOWLEDGMENTS

We are grateful to WO staff members Ezra Mashal, Friedel Loinger, Sammy Ben-Guigui, Peter Ibbetson and John Dann for their crucial contribution to this project. We gratefully acknowledge fruitful discussions with Dan Maoz and Shai Kaspi, and thank an anonymous referee for useful comments. This work is supported by the Israel Science Foundation grant 545/00.

REFERENCES

- Boller T., Brandt W. N., Fink H., 1996, *A&A*, 305, 53
 Clavel J. et al., 1992, *ApJ*, 393, 113
 Collinge M. J. et al., 2001, *ApJ*, 557, 2
 Done C., Ward M. J., Fabian A. C., Kunieda H., Tsuruta S., Lawrence A., Smith M. G., Wamsteker W., 1990, *MNRAS*, 243, 713
 Edelson R. et al., 1996, *ApJ*, 470, 364
 Edelson R. A., Krolik, J. H., 1988, *ApJ*, 333, 646
 Edelson R. et al., 2000, *ApJ*, 534, 180
 Edelson R., Turner T. J., Pounds K., Vaughan S., Markowitz A., Marshall H., Dobbie P., Warwick R., 2002, *ApJ*, 568, 610
 Gilbert K., Peterson B. M., 2003, *ApJ*, 587, 123
 Haardt F., Maraschi L., 1991, *ApJ*, 380, L51
 Haardt F., Maraschi L., 1993, *ApJ*, 413, 507
 Kaspi S., Smith P. S., Netzer H., Maoz D., Jannuzi B. T., Giveon U., 2000, *ApJ*, 533, 631
 Kotov O., Churazov E., Gilfanov M., 2001, *MNRAS*, 327, 799
 Lamer G., M^cHardy I. M., Uttley P., Jahoda K., 2003, *MNRAS*, 338, 323
 Leighly K. M. 1999, *ApJS*, 125, 297
 Leighly K. M. 1999, *ApJS*, 125, 317
 Lyubarskii Y. E., 1997, *MNRAS*, 292, 697
 Maoz D. et al., 1990, *ApJ*, 351, 75
 Maoz D., Smith P. S., Jannuzi B. T., Kaspi S., Netzer H., 1994, *ApJ*, 421, 34
 Maoz D., Edelson R., Nandra K., 2000, *AJ*, 119, 119
 Maoz D., Markowitz A., Edelson R., Nandra K., 2002, *AJ*, 124, 1988
 Mason K. O. et al., 2002, *ApJ*, 580, L117
 Nandra K., Clavel J., Edelson R. A., George I. M., Malkan M. A., Mushotzky R. F., Peterson B. M., Turner T. J., 1998, *ApJ*, 505, 594
 Nandra K., Le T., George I. M., Edelson R. A., Mushotzky R. F., Peterson B. M., Turner T. J., 2000, *ApJ*, 544, 734
 Peterson B. M., Crenshaw D. M., Meyers K. A., 1985, *ApJ*, 298, 283
 Peterson B. M., Wanders I., Horne K., Collier S., Alexander T., Kaspi S., Maoz D., 1998, *PASP*, 110, 660

- Peterson B. M. et al., 2000, 542, 161
Rodriguez-Pascual P. M. et al., 1997, ApJS 110, 9
Stern B. E., Poutanen J., Svensson R., Sikora M., Begelman M. C., 1995, ApJ, 449, L13
Shemmer O. et al., 2001, ApJ, 561, 162
Timmer J., Koenig M., 1995, A&A, 300, 707
Uttley P., McHardy I. M., Papadakis I. E., Guainazzi M., Fruscione A., 1999, MNRAS, 307, L6
Uttley P., McHardy I. M., Papadakis I. E., Cagnoni I., Fruscione A., 2000, MNRAS, 312, 880
Uttley P., McHardy I. M., Papadakis I. E., 2002, MNRAS, 332, 231
Uttley P., Edelson R., McHardy I., Peterson B. M., Markowitz A., 2003, ApJ, 584, L53
Young A. J., Crawford C. S., Fabian A. C., Brandt W. N., O'Brien P. T., 1999, MNRAS, 1999, 304, L46